Evaluation of core loss calculation methods for highly non-sinusoidal inputs

Citation for published version:
Smailes, M, Ng, C & Shek, J 2015, Evaluation of core loss calculation methods for highly non-sinusoidal inputs. in *IET International Conference on AC and DC Power Transmission.* IET.
https://doi.org/10.1049/cp.2015.0005

Digital Object Identifier (DOI):
10.1049/cp.2015.0005

Link:
Link to publication record in Edinburgh Research Explorer

Document Version:
Peer reviewed version

Published In:
IET International Conference on AC and DC Power Transmission

Evaluation of core loss calculation methods for highly non-sinusoidal inputs

[1]M. Smailes, [1]C. Ng, [1]R. Fox, [2]J. Shek, [3]M. Abusara, [4]G. Theotokatos, [1]P. McKeever

[1]ORE Catapult, UK, Michael.Smailes@ore.catapult.org.uk, Chong.Ng@ore.catapult.org.uk, Robert.Fox@ore.catapult.org.uk, Paul.McKeever@ore.catapult.org.uk
[2]The University of Edinburgh, UK, J.Shek@ed.ac.uk,
[3]The University of Exeter, UK, M.Abusara@exeter.co.uk,
[4]The University of Strathclyde, UK, Gerasimos.Theotokatos@strath.ac.uk

Keywords: HVDC, Steinmetz, iGSE, Transformer Loss

Abstract

A modular, hybrid HVDC transformer, located in the turbine nacelle has been proposed for the offshore wind industry to improve efficiency and redundancy while reducing costs. The injection of harmonics by the transformer power electronics however, complicates the core loss calculations of such a transformer. The standard Steinmetz Equation is no longer valid and the alternative loss equations proposed in the literature are significantly more complicated. Therefore, many in the industry still use the Steinmetz Equation with the signal's Fourier Transform. However, the literature suggests this to be inaccurate without quantifying it. This paper will therefore compare the accuracy of this approach to a prominent alternative presented in the literature, the improved Generalised Steinmetz Equation.

1 Introduction

The trend for offshore wind farms to move further offshore, combined with the falling cost of power electronics has resulted in an increase in the number of wind farms using HVDC systems for power transmission [1], [2]. The HVDC converters in use today though are not optimised for the offshore wind industry, offering little in terms of system redundancy and accounting for roughly 11% of their capital costs [3], [4]. A modular, high power (5-10 MW), Medium Frequency (MF = 500 – 2000 Hz), hybrid HVDC transformer (Fig 1) has therefore been proposed in [5] to address these issues. The DC bus voltage is stepped up within the turbine nacelle and converted to HVDC for parallel grid connection, negating the requirement for an offshore HVDC platform. The modular HV design increases system redundancy and inter-array cable losses are minimised. By operating in the MF range, the transformer's size and weight are minimised, simplifying the turbine's installation and foundation design.

This however, increases the transformer loss density and hence accurate calculation of core loss is imperative. Historically, transformer core losses have been calculated using the empirical Steinmetz Equation (SE) (1) but is only valid for sinusoidal waveforms.

$$p_{core} = kf^{\alpha}\hat{B}^{\beta} \tag{1}$$

Where, p_{core} is power loss per unit volume of the core (V_c), f is the frequency of the input waveform and $\hat{B}$ the peak flux density. The material constants α, β and k are collectively termed the Steinmetz Parameters. The harmonics injected by the power electronics in the hybrid transformer however, create a highly non-sinusoidal waveform, which render the results derived by applying (1) inaccurate.

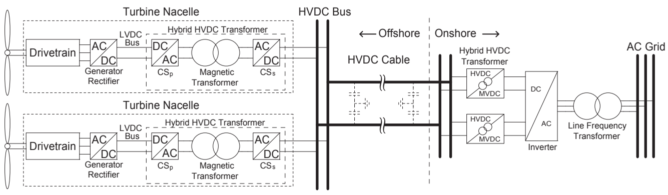

Fig 1: Offshore wind farm using proposed hybrid HVDC transformer design

Due to the recent advancements in power electronics there are now a litany of equations in the literature for calculating core loss for non-sinusoidal waveforms. These may be categorised into three areas. The first describes core loss based on either macroscopic energy calculations or statistically determining the domain wall motion. In the second, core loss is assumed to comprise of three components, hysteresis, classic eddy current loss and excess eddy current loss. While both can be accurate and indeed, separating loss components was very popular previously, many parameters are not expressly given by core manufacturers. Excessive calculations and measurements [6]–[8] must therefore be performed, thus complicating their implementation and are not discussed further here.

The third area comprises empirical formulae, which seek to generalise (1) such that it maybe used for all waveforms. The advantage of this approach is that normally only the Steinmetz Parameters are required and as such are the most practical to use. In 1999 the Modified Steinmetz Equation (MSE) [9] was published however, shortly after, the Generalised Steinmetz Equation (GSE) was released in 2001 [10] to overcome the mismatch between the SE and MSE for sinusoidal waves. The GSE was found to be less accurate than the MSE for some cases [8] though, leading to the improved General Steinmetz Equation (iGSE), published in 2003 [11]. The iGSE becomes increasing less accurate with Pulse Width Modulation however, as it does not account for relaxation effects. The improved improved General Steinmetz Equation

(i^2GSE) [12] does account for relaxation however, it requires significantly more variables, not all of which are provided by core manufacturers as standard. The iGSE is therefore considered to be the best compromise between accuracy and usability.

The iGSE however, is still significantly more complicated to implement than the SE. As a result many in the industry continue to use the SE with the Fourier Transform of the non-sinusoidal waveform (FTSE). This has been suggested to be inaccurate in the literature due to the non-linearity of the SE. The magnitude of this inaccuracy compared to the iGSE under different load cases however, has not been investigated [13].

The aim of this paper is to determine the accuracy of the FTSE and its dependence on waveform, frequency, flux density and material. For comparison, core loss will also be calculated using the iGSE and the SE. The accuracy of all three methods will be determined from experimentally obtained losses from a transformer core.

The experiment set-up is discussed in section 2 and empirical equations briefly explained in section 3. The results are displayed in section 4 and key points discussed in section 5. Conclusions are drawn on the applicability of using the FTSE in section 6.

2 Experiment Setup

There are many approaches to calculate core loss, each attempting to isolate the core losses from the winding and other parasitic losses. The set-up chosen to calculate the core losses for both characterisation and comparison purposes in this study is shown in Fig 2

A Pacific 360-AMX power generator was used to generate 5 test waveforms to investigate how accuracy changes with wave shape. The waveforms used shown in Fig 3 include: a sine wave; distorted sine wave at 10% Total Harmonic Distortion (THD); a triangular wave and two square waves at 0.33 and 0.5 duty ratios (D=0.33 and D=0.5 square). Each waveform was repeated over a range of frequencies between 500 Hz and 2,000 Hz and voltages 20 V_{rms} and 60 V_{rms} to test for sensitivity to both f and B. The generated waveform was verified by a Voltech PM6000 Universal Power Analyser and fed to the primary winding of the Core Under Test (CUT). Ferrite was chosen as the core material as this is a realistic material for this application, while still exhibiting enough losses to yield accurate results. The CUT was placed in a Weiss Technik SB Series environmental chamber set to 25 °C to maintain constant ambient conditions. A thermocouple, attached to the CUT logged its temperature to ensure a constant core temperature is maintained throughout testing.

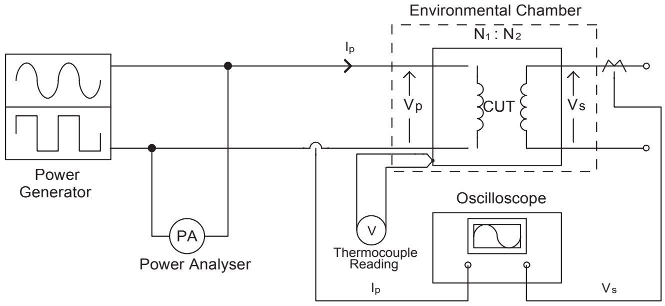

Fig 2. Core loss experiment setup

The secondary winding of the transformer was open circuited and 4 cycles of the primary current and secondary voltage recorded using a Tektronix TDS 2024B oscilloscope. By measuring the open circuit secondary voltage, only the core losses were considered, allowing the direct calculation of the BH loop. This method is widely used in the literature due to its accuracy. Flux Density (B) can then be calculated from:

$$B = \frac{1}{N_2 A_e}\int_0^{\tau} v(t)dt \tag{2}$$

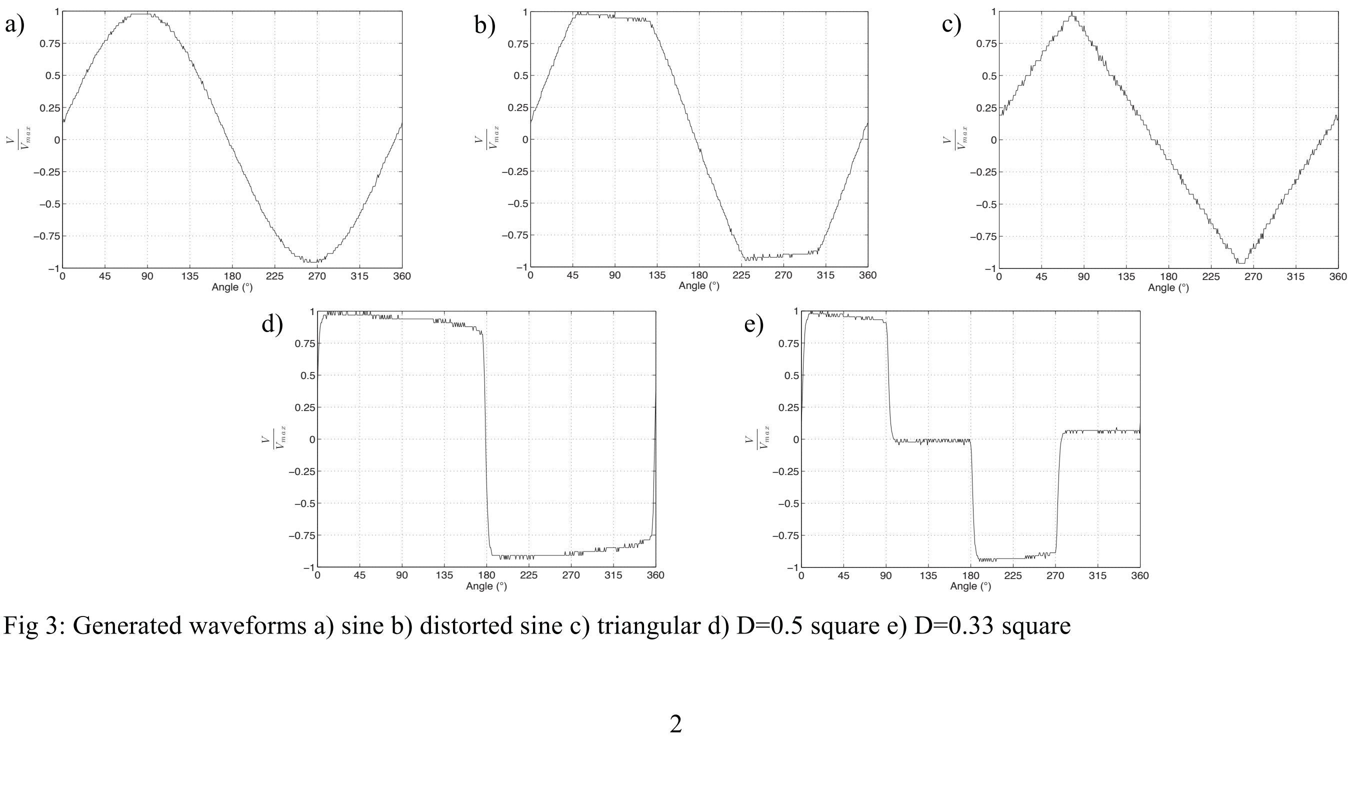

Fig 3: Generated waveforms a) sine b) distorted sine c) triangular d) D=0.5 square e) D=0.33 square

Where N_2 is the number of turns on the secondary, A_e is the effective area of the core and $v(t)$ is the time varying voltage across the secondary. The magnetic field strength (H) is then defined as:

$$H(t) = \frac{N_1 i(t)}{L_e} \tag{3}$$

Where N_1 is the number of turns on the primary $i(t)$ is the time varying primary current and L_e the magnetic path length.

The core power loss per unit volume is:

$$p_{core} = f \oint B \cdot dH \tag{4}$$

Where f the waveform frequency.

The core manufacturer's datasheet only provides core loss information between frequencies of 25 kHz to 400 kHz. The range of interest however, lies far outwith of this at 500 Hz to 2000 Hz. Therefore the CUT needed to be characterised first to determine its Steinmetz Parameters over the range of interest. To accomplish this, sine waves between 500 Hz and 2000 Hz at flux densities of 0.05 T to 0.3 T were passed through the CUT. H was then calculated using (3) and the core loss from (4). These results were then extrapolated to cover frequencies up to 4 kHz. Extrapolating the loss data from the datasheet covered the remaining 4 kHz to 10 kHz and 10 kHz to 25 kHz frequency ranges. The properties of the CUT are given in Table 1.

Manufacturer	Epcos
Material	N87 Ferrite
Shape	UI
L_e (m)	0.258
A_e (m^2)	8.4×10^{-4}
N_1:N_2	92:37
V_c (m^3)	2.17×10^{-4}
B_{sat} (T)	0.49

Table 1: CUT property table

A three dimensional linear regression of the logarithm of (1) using the relationship between core loss, frequency and flux density can then be used to calculate the Steinmetz Parameters for the frequency ranges shown in (Table 2).

Frequency Range (Hz)	**Core 1**		
	k	α	β
<1000	49.580	1.194	2.265
1000-4000	26.682	1.286	2.295
4000-10,000	267.213	0.774	1.472
10,000-25,000	1029	0.763	1.952
25,000-50,000	398.87	0.921	2.200
>50,000	71.305	1.114	2.338

Table 2: Calculated Steinmetz Parameters

3 Predicted Core Loss

With the calculated Steinmetz Parameters core loss may be calculated using the three analytical methods: the SE, FTSE and iGSE for each experiment variation. As several cycles were recorded for each variation these were first separated into individual waves for the SE and iGSE methods. The average core loss for each variation was then taken to improve accuracy. The SE can therefore be simply calculated from (5), which has been adapted from (2).

$$p_{core} = \frac{1}{n}\sum_{i=1}^{n} k f_i^{\alpha} \hat{B}_i^{\beta} \tag{5}$$

For the i^{th} of n cycles in each experimental variation.

To find the core loss through FTSE, the Fast Fourier Transform (FFT) of B must first be found to separate it into its harmonic components. The SE can then be applied to each component (j to m) and summed using vector addition to determine the total core loss according to (6). As only 4 cycles could be recorded on the oscilloscope, the flux density vector was first extended ($\hat{B}ext$) to improve the FFT accuracy. This was achieved by repeating the recorded cycles, taking great care to stich the repeated cycles together properly so that the end of the last sequence lead into the beginning of the next.

$$p_{core_i} = \sqrt{\sum_{j=1}^{m}\left(k_j f_j^{\alpha_j} \hat{B}ext_j^{\beta_j}\right)^2} \tag{6}$$

Application of the iGSE however, requires B to be passed through an algorithm first. The algorithm must separate B into its rising and falling sections and then major and minor loops and if necessary, the minor loops into sub-loops and sub-sub-loops etc. A rising minor loop, or minor sub-loop is defined as; a period when the flux density decreases in an area where the average gradient is positive until the original flux density (before the decrease) is reached. The major loop then, contains all the data points in the rising section, minus those contained in the minor loop so that the major loop is monotonically increasing. The same can be applied to the falling section of the B-H curve. The iGSE should then be applied to each loop and summed to find the total power loss for the cycle as in (7)-(9).

$$k_{iGSE} = \frac{k}{(2\pi)^{\alpha-1} \cdot 2^{\beta-\alpha} \int_0^{2\pi} |cos\theta|^{\alpha} d\theta} \tag{7}$$

$$p_{loop} = \frac{1}{T}\int_0^T k_{iGSE} \left|\frac{dB}{dt}\right|^{\alpha} (\Delta B)^{\beta-\alpha} dt \tag{8}$$

or, as a discrete function:

$$p_{loop} = \frac{k_{iGSE}\Delta B^{\alpha-1}}{T}\sum_{l=1} \left|\frac{\delta B_l}{\delta t_l}\right|^{\alpha} \delta t_l \tag{9}$$

Total core loss is then determined by a weighted average of the power from each loop as in (10) and the average loss from each variation calculated by applying (11).

$$p_{core_i} = \sum_{o=1}^{q} P_o \frac{T_{loop_o}}{T_{cycle}} \tag{10}$$

$$p_{core} = \frac{1}{n} \sum_{i=1}^{n} p_{core_i} \tag{11}$$

Where p_{loop} is the core loss for each loop, δB_l is the change in flux between points l and l-1, δt_l is the time between point l and l-1 and T_{cycle} and T_{loop} are the periods of the cycle and the o^{th} *loop* respectively. The results of all three methods may then be compared to the experimentally obtained core losses and hence the accuracy of each determined.

4 Results

The calculated core losses for the Epcos N87 core are presented here. The results are analysed for; constant input voltage, varying frequency and flux density; constant frequency, varying voltage and flux density; as well as constant flux density, varying voltage and frequency (2). The losses were calculated using experimentally obtained voltage and current measurements and three empirical methods; the standard SE, the FTSE and the iGSE. The measurements and calculations were repeated for five waveforms; a sine wave, distorted sine wave with a 10% THD, a triangular wave and two square waves, D=0.33 square and D=0.5 square. The results are shown below in Fig 4 to Fig 6.

It can be seen from Fig 4 to Fig 6 that all three empirical methods achieved the best results when used with a sinusoidal input voltage waveform. This is particularly true for the constant frequency case. It is clear that as the THD of the input waveform increases towards 45% (the D=0.5 square wave), the accuracy of the standard SE diminishes. This is to be expected as the SE is only valid for sinusoidal waveforms.

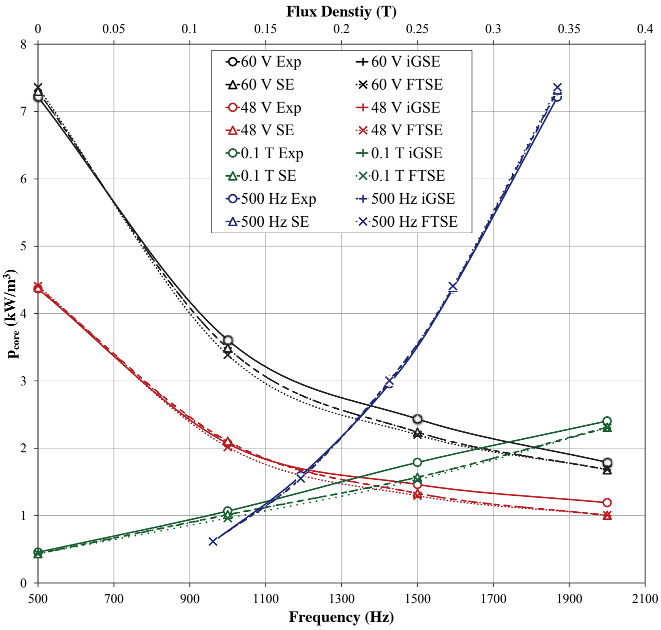

Fig 4: Core losses for a sine wave determined from experimental results, the SE, FTSE and iGSE at different frequencies and flux densities.

To compensate for this inaccuracy many in the industry perform a Fourier Transform on the flux density waveform and use the SE on the result. This approach yielded relatively accurate results for the sinusoidal, distorted sinusoidal and triangular waves over all frequencies and flux densities but performed best at lower flux densities and frequencies.

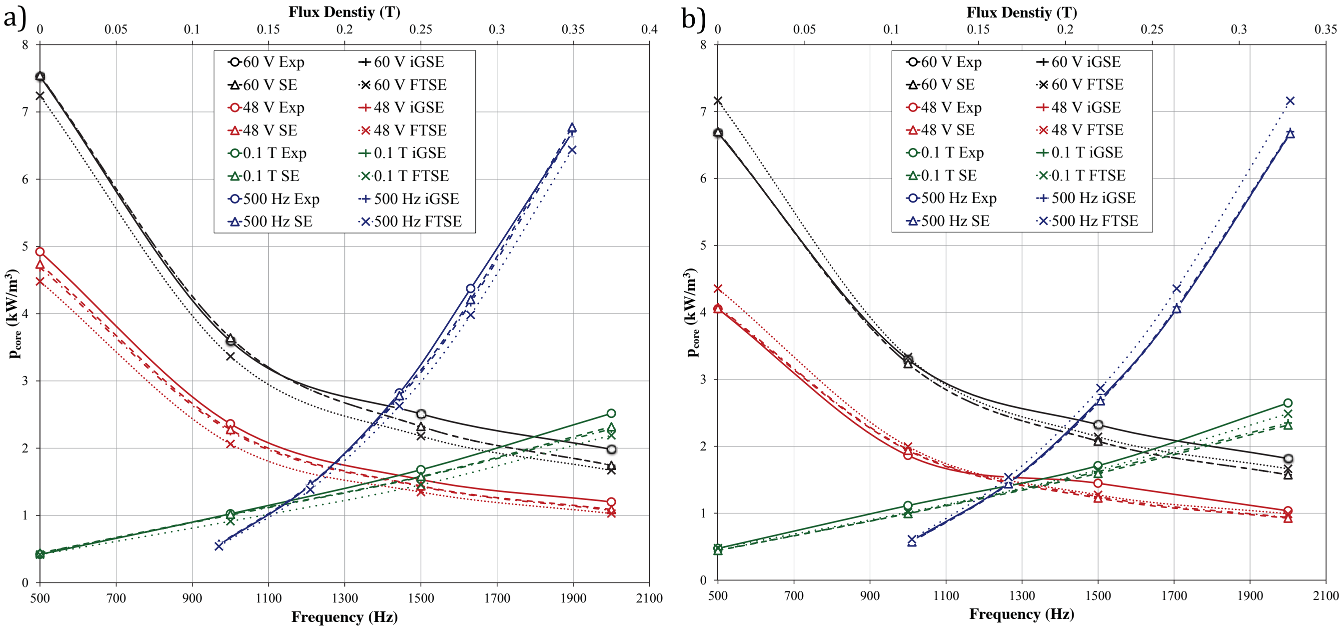

Fig 5: Core losses for a) distorted (10%THD) sine wave and b) triangular wave determined from experimental results, the SE, FTSE and iGSE at different frequencies and flux densities.

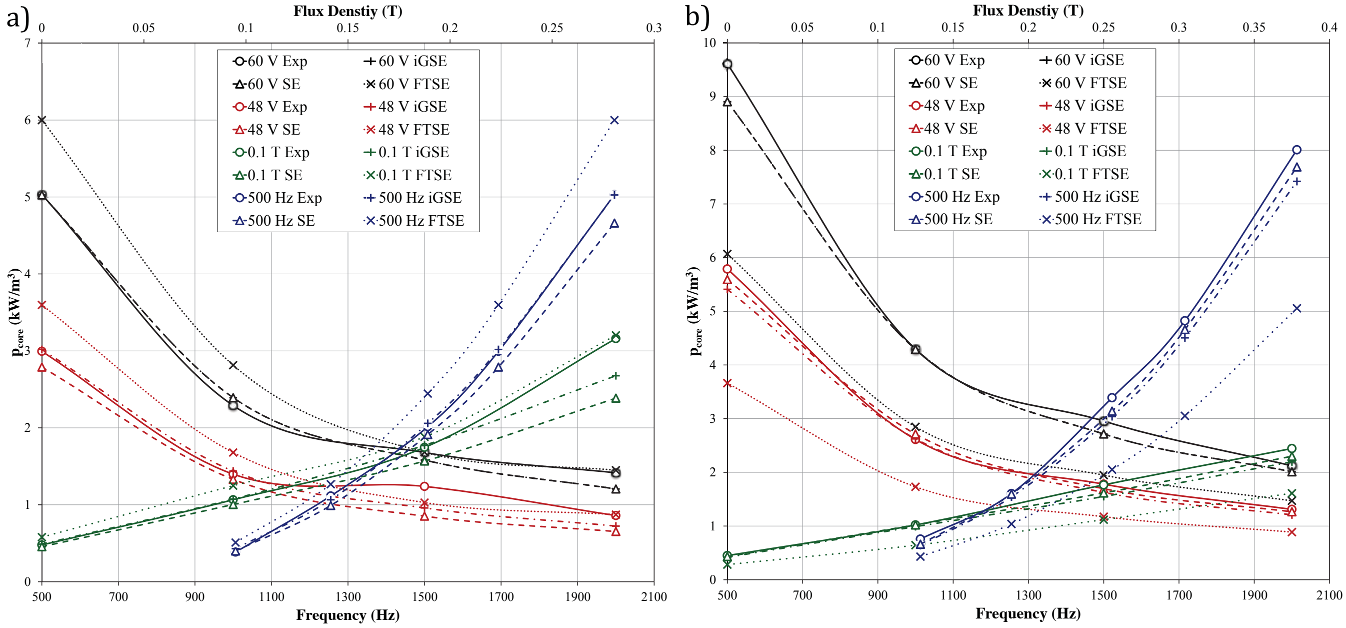

Fig 6: Core losses for a) square wave (D=0.33) and b) square wave (D=0.5) determined from experimental results, the SE, FTSE and iGSE at different frequencies and flux densities

The iGSE performed well over all waveforms, frequencies, voltages and flux densities, matching the experimental data best in all but the D=0.5 square wave. Here, somewhat surprisingly the standard SE performed marginally better. Both the SE and FTSE performed best between 500 Hz and 1000 Hz achieving errors of around ±5% for the sinusoid, distorted and triangular waveforms. The iGSE continued to perform well for the D=0.33 square wave with errors <±5% but this increased for the D=0.5 case to around ±7%. The SE had errors of ±5% for the D=0.5 square wave however, this increased to ±8% for the D=0.33 square wave.

The error of all methods increased for frequencies above 1000 Hz, in some cases by a factor of 2. However, this is likely due to a poorer fit of the calculated Steinmetz Parameters with the calibration results and is discussed further in section 5. This does however, highlight the importance of obtaining accurate Steinmetz Parameters. A Safety Factor (SF) of around 5% should be used if there is a high degree of confidence in the values of the Steinmetz Parameters and otherwise a SF of 10% should be used with the SE and iGSE methods. While the error of the FTSE is similar to that of the SE and FTSE for the sinusoid and triangular waves, it increases to around ±45% in the square wave cases.

In both constant voltage sets (60V and 48V) the power loss decreases with increasing frequency. This is due to the peak flux density decreasing with frequency (2). It can be seen from Table 2 that the flux density exponent, β, is greater than that of frequency, α, resulting in an inverse relationship with frequency. If either flux density or frequency is held constant, the power loss increases with increasing frequency and input voltage respectively.

5 Discussion

As can be seen from Fig 7 the Steinmetz Parameters obtained for frequencies below 1 kHz offered a closer fit to the measured core losses for all flux densities. The consequence of this can be seen in the experiment results presented in Fig 4 to Fig 6 but is particularly evident for the sinusoidal case in Fig 4. Here it can be seen that at the lower frequency end of the constant voltage and constant flux density waveforms, the error in the empirical calculations is smaller. Better results were also achieved from the constant frequency sets as they were taken at 500 Hz.

It can also be seen in Fig 7 that the core behaves oddly around 1.5 kHz. This point was retested and the results proved repeatable. Extra data points were then taken around it showing a trend towards it further validating this point. The cause of this deviation from the trend at 1.5 kHz is unclear but as it occurs for all flux densities and proved repeatable, the results suggest it is due to a quirk in the core rather than measurement error. The consequence of this is the reduced accuracy of the empirical equations around this frequency and the general reduction in accuracy above 1000 Hz.

While the error of the SE and FTSE in the triangular wave case was surprisingly low, it can be explained as follows. The SE is based on the flux density waveform not that of the voltage waveform and from (2) the flux density is obtained from the integral of voltage. The resulting waveform is therefore sinusoidal with a relatively low THD. Waveforms with a low THD are often used with the standard SE resulting in a relatively accurate representation of core losses for both the 10% THD and triangular waveforms.

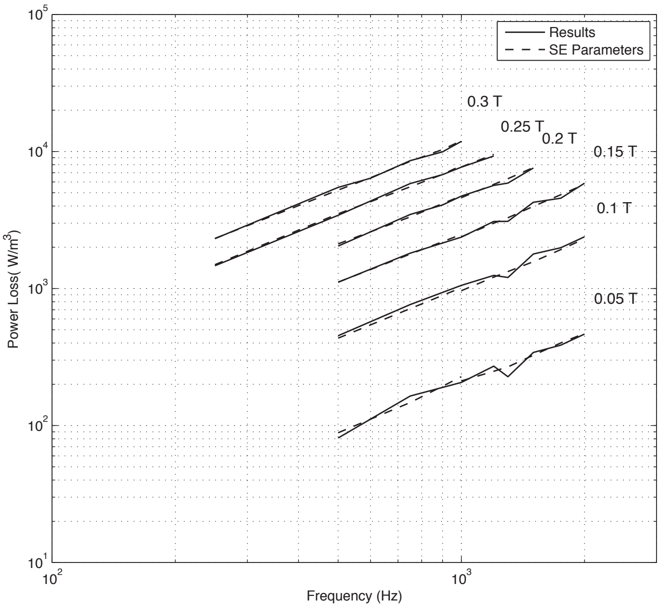

Fig 7: Measured core loss between 500 Hz and 2000 Hz and 0.05 T and 0.3 T with corresponding core loss predicted by Steinmetz Parameters

As evident in Fig 6a. & Fig 6b the FTSE becomes highly inaccurate, less so even than the standard SE. While the literature suggests that it would be inaccurate due to the non-linearity of the SE, the extent of the error was still surprising. Further investigation revealed that, while the FFT picked out the correct frequencies of each harmonic, the magnitude of the components differed significantly from the original waveform in the square wave cases. As the flux density is raised to a power between 2.2 and 3 (Table 2) in the SE this error is magnified, significantly affecting the results. It is known that the component magnitudes are often less accurate than their frequencies and many windowing techniques exist to improve its accuracy. It is possible therefore that better results maybe obtained though applying an appropriate window to the results. Increasing the resolution of the measurement data may also improve the results, although voltage and current readings were already taken at the relatively high frequency of 0.25 MHz to 1 MHz.

It is thought that the source of this inaccuracy is the requirement of an infinite number of harmonic components to accurately represent the energy contained in each component of highly non-linear flux density waveforms generated by square waves. Since it is not possible to create an infinite number of harmonics, the energy is incorrectly distributed across them, leading to an error in the magnitude of the attributed flux densities.

It might be expected that the accuracy of the iGSE for the D=0.33 case would decrease compared to that of the D=0.5 case due to relaxation effects. From Fig 6 however, this does not appear to be true as the error increases for the D=0.5 case. This may be because the increase in error caused by the effect of magnetic relaxation is small compared to that caused by the increase in THD in this example. The balance may well shift though if the number of rapid changes in the core's magnetization is increased, such as would be experienced due to pulse width modulation.

6 Conclusion

The Steinmetz Equation is used extensively in industry in conjunction with a Fourier Transform to calculate losses in non-sinusoidally excited transformer cores. This paper compared the accuracy of this approach to using the Standard SE and iGSE by comparing the calculated core losses to those measured in an Epcos N87 ferrite core. The core was tested under different waveforms to investigate the effect frequency, flux density, voltage magnitude and wave shape has on the accuracy of each empirical method.

All three methods were found to be most accurate for a sinusoidally excited core. The FTSE was found to also be relatively accurate for a 10% THD sinusoid and triangularly excited core particularly at low flux densities but relatively inaccurate for both square waves tested. Overall the iGSE was found to be the most accurate, although the accuracy slightly reduced for the D=0.5 square wave. The iGSE is therefore recommended for highly non–sinusoidal flux density waveforms in preference to using the FTSE.

Acknowledgements

The authors would like to thank the ETI and RCUK Energy programme for IDCORE (EP/J500847/1) as well as the Technology Strategy Board for their funding and Dr Mark Knos for his support

References

[1] B. Van Eeckhout, D. Van Hertem, M. Reza, K. Srivastava, and R. Belmans, "Economic comparison of VSC HVDC and HVAC as transmission system for a 300 MW offshore wind farm," *Eur. Trans. Electr. Power*, pp. 661–671, Jun. 2009.

[2] A. Arapogianni, J. Moccia, J. Wilkes, J. Guillet, P. Wilczek, J. Scola, and S. Azau, "The European Offshore Wind Industry - Key Treds and Statistics 2012." European Wind Energy Association, Jan-2013.

[3] "Offshore Wind: Nordzee Ost," Oct-2013. [Online]. Available: http://ec.europa.eu/energy/eepr/projects/files/offshore-wind-energy/nordsee-ost_en.pdf. [Accessed: 18-Feb-2014].

[4] P. Giller, "Multi-Contracting for the first project financing in the German Offshore Wind Market: Projekt Offshore Wind Farm Meerwind Sud/Ost [288 MW Offshore Wind Farm]," 03-Jan-2012.

[5] C. Ng and P. McKeever, "Next generation HVDC network for offshore renewable energy industry," in *10th IET International Conference on AC and DC Power Transmission (ACDC 2012)*, Birmingham, 2012, pp. 1–7.

[6] G. Bertotti, "General properties of power losses in soft ferromagnetic materials," *IEEE Trans. Magn.*, vol. 24, no. 1, pp. 621–630, 1988.

[7] P. A. Hargreaves, B. C. Mecrow, and R. Hall, “Calculation of iron loss in electrical generators using finite element analysis,” in *Electric Machines & Drives Conference (IEMDC), 2011 IEEE International*, 2011, pp. 1368–1373.
[8] I. Villar, U. Viscarret, I. Etxeberria-Otadui, and A. Rufer, “Global Loss Evaluation Methods for Nonsinusoidally Fed Medium-Frequency Power Transformers,” *IEEE Trans. Ind. Electron.*, vol. 56, no. 10, pp. 4132–4140, 2009.
[9] J. Reinert, A. Brockmeyer, and R. W. A. A. De Doncker, “Calculation of losses in ferro- and ferrimagnetic materials based on the modified Steinmetz equation,” *IEEE Trans. Ind. Appl.*, vol. 37, no. 4, pp. 1055–1061, Jul. 2001.
[10] J. Li, T. Abdallah, and C. R. Sullivan, “Improved calculation of core loss with nonsinusoidal waveforms,” in *Industry Applications Conference, 2001. Thirty-Sixth IAS Annual Meeting. Conference Record of the 2001 IEEE*, 2001, vol. 4, pp. 2203–2210.
[11] K. Venkatachalam, C. R. Sullivan, T. Abdallah, and H. Tacca, “Accurate prediction of ferrite core loss with nonsinusoidal waveforms using only Steinmetz parameters,” in *2002 IEEE Workshop on Computers in Power Electronics, 2002. Proceedings*, 2002, pp. 36–41.
[12] J. Mühlethaler, J. Biela, J. W. Kolar, and A. Ecklebe, “Improved core-loss calculation for magnetic components employed in power electronic systems,” *IEEE Trans. Power Electron.*, vol. 27, no. 1, p. 964, 2012.
[13] M. Albach, T. Durbaum, and A. Brockmeyer, “Calculating core losses in transformers for arbitrary magnetizing currents a comparison of different approaches,” in *, 27th Annual IEEE Power Electronics Specialists Conference, 1996. PESC ’96 Record*, 1996, vol. 2, pp. 1463–1468 vol.2.